

RUNNING TITLE: Probability maps in visual cortex

'Spatial probability maps in primary visual cortex' vs. 'Attention violates Bayesian expectations in primary visual cortex'

Scott G. Warren¹, Geoffrey M. Ghose^{1,2}

¹Department of Neuroscience, University of Minnesota, Minneapolis, MN, USA;

²Center for Magnetic Resonance Research, University of Minnesota, Minneapolis, MN, USA;

***Correspondence:**

Geoffrey M. Ghose
Center for Magnetic Resonance Research
University of Minnesota
2021 6th St SE
Minneapolis, MN USA 55455
ghose@umn.edu

Abstract

We live in an uncertain world, and efficient decision making in such a world requires understanding that uncertainty and making use of it. While numerous behavioral and modeling studies have suggested that perceptual judgments incorporate estimates of stimulus uncertainty, the physiological mechanisms of this incorporation, and correspondingly, the physiological constraints on likelihood-based judgments remain unclear. To address this issue, we trained monkeys in a challenging visual detection task in which target probability consistently varied over visual space throughout training. We designed this task such that the spatial extent of targets, and the spatial variation in probability, was on a very fine scale on the order of a receptive field in primary visual cortex. We found that behavioral performance tended to be better for high probability locations, but the spatial correlation between performance and probability was imperfect, with relatively coarse spatial variations in performance. To study the physiological basis of such spatial performance variations we measured activity patterns across cortex during task performance using intrinsic flavoprotein autofluorescence imaging. We found that the correlation between spatial performance and the spatial pattern of V1 activation was strong, and was maintained even when the spatial probability schedule was altered. Together, these results suggest that, even in the earliest levels of sensory representation, stimulus likelihood modulates activity through feedback connections and that, for tasks

requiring analysis at an early level, the precision and magnitude of these modulations are largely responsible for the effects of probability on performance.

Introduction

Numerous theoretical and behavioral studies have shown that perceptually based actions rely on the preferential processing of sensory signals according to their likelihood, yet the physiological mechanisms of how likelihood is represented and integrated with sensory signals remain uncertain. For example, likelihood could modulate sensory signals directly, or, alternatively, bias the readout or decoding of such sensory signals. One clue to the potential mechanism is the large number of studies demonstrating that sensory signals can be directly modulated by instructing subjects to selectively attend to a particular location or object. However, because these studies have largely used unambiguous cues to direct attention in a binary way towards or away from a particular location or object, they have been unable to examine if, or how, inferred probabilities arising from experience directly modulate sensory signals in the brain.

To study this issue requires a probabilistic task in which behavior is consistent with a direct modulation of sensory signals. One such task is the detection of spatially localized changes in which performance reflects variations in target probability across visual space. Because this biasing occurs automatically, without awareness, and with high spatial resolution, it suggests that probability signals might be present in the very earliest levels of visual processing within the cortex. To directly test this hypothesis, we trained monkeys in a challenging detection task in which the spatial probability of target appearance varied

on the scale of V1 receptive fields. We found that, after such training, detection performance across visual space was correlated, but not perfectly, with target probability. We then measured the distribution of stimulus evoked activity across primary visual cortex using invasive optical imaging [1] while monkeys performed this detection task. We found that visual responses across the cortex were well correlated with the spatial pattern of detection biases, and that these cortical activation biases flexibly shifted, as did the behavioral detection biases, when animals were trained with a new probability structure. In all cases, both the behavioral biases and activity modulations were on a coarser spatial scale than the probability variations, suggesting that the structure and distribution of feedback projections to V1 is a primary constraint to fine scale spatial probability representations.

Results

Detection of changes in V1-scaled stimuli

We trained two rhesus macaques to detect the brief, perceptually faint contrast increment of the single Gabor elements positioned within a 3x3 array of stimuli (Fig. 1). The size of the individual elements was 1-1.25 times the size of V1 receptive fields at the stimulated eccentricity (Monkey F: 0.15°; Monkey P: 0.2° radius), as estimated from known V1 electrophysiology [2], and the array was simple-cubic close-packed such that the individual elements lay in the surround fields of their neighbors. All other Gabor

parameters were chosen to maximally activate local V1 neurons. Both animals maintained within $\pm 0.5^\circ$ fixation to a 0.125° target circle, with median single trial eye position variance less than the stimulus element size (50/95th percentile: Monkey F: $0.148^\circ/0.222^\circ$, Monkey P: $0.106^\circ/0.195^\circ$).

Two stimulus arrays were presented in opposite hemifields, and the hemifield in which changes were likely to occur was explicitly cued with instruction trials. Both subjects readily followed this left/right cue between hemifields: sensitivity to detect increments in the cued hemifield was substantially greater than in the uncued hemifield (Monkey F: 64% versus 34%; Monkey P: 83% versus 38%; $p < 0.05$ in both subjects, binomial distribution, variable DOF).

To study the effects of probability on visual responses and behavior, we manipulated the probability that the increment would occur at a given stimulus position within each array. In both animals, one position close to the fovea and one position further in the periphery (separated by Monkey F: 0.85° ; Monkey P: 1.13°) were each eight times more likely to host the contrast increment than were the other seven positions (Fig. 1). The bias locations were fixed and never explicitly instructed to the subjects, but rather were trained over weeks of repetition. In behavioral training prior to physiologic measurements, both animals showed a relative increase in detection sensitivity toward one or both biased stimuli. To avoid position-specific perceptual learning effects, this training occurred in the peripheral upper hemifield far from the expected representation of the imaged V1.

After training with appropriately scaled stimuli, we found that both animals enjoyed a modest benefit to detecting increments at the two biased locations relative to the 7 more central locations (Fig. 1). The overall sensitivity to bias-matched increments was higher (Monkey F: +17% Monkey P: +13%; $p < 0.01$ at both bias locations in both subjects, binomial distribution confidence intervals, variable DOF) and the reaction time of saccades to biased-match increments was lower (Monkey F: -4.6 ms; Monkey P: -7.4 ms, $p < 0.05$ at both bias locations in P and in peripheral bias location in F, t -test, variable DOF). The match between behavior and stimulus probability was however not perfect. The pattern of behavioral performance on the individual bias-mismatched elements (Fig. 4) strongly suggests that both subjects struggled to attend focally on only the bias targets. Either some attentional resources spilled into neighboring elements, or read-out effects in later visual areas impaired V1 attentional targeting, in a subject-specific pattern. The individual behavioral patterns will be explored in combination with imaging data later in this report.

Because of the imprecision in behavioral performance and because these data are averages derived from hundreds of trials, we can not conclude that the subjects are simultaneously splitting attention to two distinct foci, a topic of controversy [3]. It is possible, for example, that the subjects rapidly alternated attention between the two biased locations. We more conservatively concluded that each subject's performance was influenced by probabilities in a subject specific manner, and we then asked whether modulations reflecting this influence may be found in V1.

Physiologic Response to Individual Stimuli

Our primary objective was to explore the effect of probability on the V1 representation of each individual stimulus element. This required us to first carefully measure the V1 visually-evoked response to each single element of the stimulus array when presented in isolation. After mapping the retinal topography of the imaged region of V1 using standard methods, we determined that the chamber of one subject (Monkey P) was placed over the approximate region of V1 that was expected from known macaque V1 anatomy in the close peripheral lower hemifield (Fig. 1). However, the other subject (Monkey F) showed strong visual responses only when the stimulus was placed near the fovea. In Monkey F, we therefore used smaller stimuli which were more closely packed. We also used a higher base contrast when mapping his chamber as these foveal signals were initially difficult to detect.

After the retinotopic location of the chamber was determined, subjects performed the same task as above except only one element was displayed on a given trial (this element was always the location of the contrast increment, so no selective attention was required). Notably, both subjects were unable to detect contrast increments at singly-presented locations with the same threshold for which they could be detected in the whole array—both subjects required stronger singleton contrast increments to perform the task (data not shown, this calibration was performed quickly online). This difference in contrast

increment threshold can not be explained by integrating signal over the entire array.

Rather we concluded that both subjects solve the array task by comparing the relative contrast of neighboring stimuli, which requires spatial integration and comparison operations to be performed on the scale of the individual stimuli (on the scale of V1 neural receptive fields).

While both subjects' V1 showed a robust visually-evoked response to the array and to single elements, we found large differences in the spatial precision of single-target responses between animals. In Monkey P, consistent with past literature, we found that each stimulus element evoked a V1 response within a small locus (Fig. 2a). The individual element evoked-responses were modest early in the trial, but were well-defined by a strongly negative hemodynamic signal late in each trial. This late, negative signal has been described previously [4], and we verified its hemodynamic nature with a separate series of red-illuminated images measuring the intrinsic hemodynamic signal [5]. The location of this well-defined response moved appropriately along the V1 cortical surface as the different singleton stimuli were presented. We also observed a strong and diffuse surround signal that typically co-localized with nearby blood vessels. These regions of hypervasculature response were masked out and not considered in future analysis. Thus we were able to unambiguously define a small region of V1, approximately 1mm in diameter, associated with each individual stimulus element.

In Monkey F, each singleton stimulus evoked a stronger but more diffuse response over the entire imaging window. This response matched the expected time course of AF activity (with onset <500ms after stimulus presentation) and did not demonstrate the negative response associated with broader hemodynamic signals. We interpreted this diffuse response as a real AF signal that may be due to the more foveal location of his chamber, the closer packed or higher contrast stimuli we used for this subject, or due to blurring of the V1 signal due to the need to image his V1 through an arachnoid neomembrane.

None-the-less, while ideal retinotopy was not recovered from Monkey F's chamber, we observed unique patterns of activity from the early period of each singleton's visually evoked response. In both animals, positional responses were distinguishable as quickly as 200 ms after stimulus onset (Fig. 2).

The poor retinotopy of Monkey F's chamber prevented us from using a simple region-of-interest analysis for each position. However, as noted, single target response patterns across the chamber for each subject were distinguishable. Thus, as animals performed their full task with the composite stimulus array we were able to decompose V1 activity to the full array into a linear sum of the activity to each singleton using a multiple linear regression model where the regression β -statistics indicate the extent to which each singleton's V1 representation contributes to a composite-stimulus response. In these future analyses, we performed the regression only using pixels contained within a single manually defined region-of-interest (ROI) that included visually responsive center

and surround pixels from all nine stimulus elements while discarding regions of the chamber corrupted by blood vessels, image artifacts, or implant material.

Physiologic measurement of response modulations in V1

After singleton V1 responses were measured, subjects performed the contrast increment detection task on the full array of stimuli with left/right cues and the positional bias present. After discarding trials that ended earlier than 1 second, in which fixation was broken, in which large motion artifacts occurred, or in which uncorrectable software/hardware errors caused data loss, we were left with 2733 full attention task repetitions (F: 1005, P: 1728). The difference in trials is due to a greater tendency of Monkey F to make an early false positive report- in comparing the two subjects we always first compute and then compare inter-subject means, so P is not over-represented in our analyses. The behavioral dataset presented in Figure 1 used the all available data from each animal, but the positional behavior described here uses only this restricted subset of trials. Because of the sparse sampling of unbiased targets, some noise in the estimation of behavior for each position was tolerated. Importantly, we only analyze trials collected before a saccade or a contrast increment occurs- the visually evoked signal from contrast increments (which we estimated to be real but minuscule, not shown) does not influence our measurement of pre-increment attention activity.

In the early trial period (600-1600ms post-stimulus onset), both animals showed a net increase in the AF signal across the V1 ROI when attention was directed contralateral to the imaged V1 hemisphere (Fig. 3), $p \approx 0$, t -test, DOF >3 million pixels \times repetitions per animal at each time point). Later in the trial, the time course of chamber-wide activity remains distinct between the two attention conditions in both animals. However, in Monkey P the sign of this difference inverts as his stronger hemodynamic signal washed out the early AF signal. As it is known that the early stages of the combined AF/hemodynamic signal better reflect AF signal and are spatially more precise [4], we limit our analysis to the early attention period to avoid ambiguity in the sign of attentional modulations in the late in the trial (as both AF signal decrease and hemodynamic signal increase appear as a negative signal change).

On visual inspection, the mean two-dimensional pattern of early attentional enhancement over hundreds of trials has multiple clear peaks in each animal. We do not, however, claim that the animals are simultaneously attending to two locations- multifocal attention is controversial and we can not distinguish between a truly multifocal modulation versus other strategies such as attending to a continuous subset of the array or rapidly changing attentional allocations throughout the trial ("flipping" attention over multiple foci). Rather, we only interpret this non-uniform distribution as evidence that modulations associated with probability were targetable to only a subset of the V1 on the order of the size of the

representation of individual stimuli. This implies that such modulations within V1 may be targeted to as little as 0.5° of visual space.

Using the previously-measured singleton activity, we decomposed the map of attentional modulations for each animal into an attention vector of gain modulations for each individual element (Fig. 4). We chose to model attention as a multiplicative gain because this type of modulation has been reported in several studies in V1 and other cortical areas. Moreover, gain modulations can explain numerous results of seemingly greater complexity by carefully modeling the effect of appropriate gains within non-linear neural networks.

Because our analysis regresses attention against the raw evoked activity from each singleton, it normalizes the magnitude of the attentional modulations by the magnitude of evoked visual responses. While Figure 3 suggests that the two subjects had vastly different cued attention modulation amplitudes, our regression analysis suggests that the amplitude of modulations attributable to probability is similar between subjects ($\pm 30\%$).

This is because our decomposition regression includes a constant term so that non-specific attentional modulations are controlled in both subjects; this term is considerably larger in Monkey F than in Monkey P (Fig. 4). While this may be due to individual differences in their stimulus configuration, overall task difficulty, or attention strategies, both subjects performed similarly and significantly worse on detecting cue-invalid targets in the

non-attended hemifield (Monkey P: $38 \pm 13\%$, Monkey F: $32 \pm 20\%$, binomial distribution 95% confidence interval) than for cue-valid targets (P: $83 \pm 3\%$, F: $64 \pm 4\%$).

In order to compare the positional distributions of both response modulations and detection performance, we first need to remove the effect of the probability distribution from each data set. This is because, plausibly, the biases could be implemented anywhere in the brain and have similar but independent effects on both distributions. By regressing the probability distribution out from both our behavioral and physiologic data, we better assess whether attentional modulations in V1 directly correlate with behavior. In Monkey F (but not P, who had larger and more peripheral stimuli), we also found that a simple surround suppression model also significantly correlated with behavior (see Table 1). Thus we added to our partial correlations a surround suppression term, but the magnitude of this regressor was set to 0 for Monkey P.

Having regressed out the effects of the probability distribution, we found that high probability positions had greater stimulus sensitivity (partial correlation, $r^2 = 0.51, p = 0.001$) after correcting for the influence of the probability distribution (and surround suppressive effects in Monkey F) on both distributions. We also observed a very weak trend toward reductions in reaction time ($r^2 = 0.06, p = 0.34$). In neither subject do the maps of behavior or attention perfectly reflect the trained probability bias toward two location. These differences are unsurprising, as the perceptual decision of whether an increment occurred relies on several further stages of cortical processing throughout the

visual and oculomotor systems. It is plausible that attentional modulations, intraareal computations, and readout factors between other areas will non-uniformly effect processing of different stimulus elements. In the greater context of the entire visuomotor response, it is remarkable that as much as half of the positional differences in mean stimulus sensitivity may be explained by appropriately-matched V1 attentional modulation.

V1 modulations promote new behavior after task perturbation

Although we found a strong correlation between V1 modulation and stimulus sensitivity on a scale of less than 0.5 visual degrees, it remained unclear that this correlation represents the output of a flexible modulatory system based on task probabilities. First, the overall match between probability and performance is crude when viewed over all nine positions (see Table 1 in Methods). For example, Monkey F clearly misdirects his performance toward a bias-mismatched foveal location (Fig. 4, far left stimulus position). It is not clear whether such mismatches reflect true modulatory imprecision, poor task comprehension, or task-invariant phenomenon such as the effects of normalization [6], surround suppression [7], or crowding [8] on V1 neuron responses. Second, recall that both subjects were exposed to the same positional bias for months of training. Although these data were collected from an untrained region of the visual field and thus we did not

over-train the imaged region of V1, we may have yet trained higher-level, position-invariant attentional allocations to this bias pattern.

To test this, we abruptly changed the bias distribution for each subject. In Monkey P we rotated the probability distribution, while in Monkey F we removed the bias completely and presented a uniform distribution (Fig. 6). Both animals behaviorally responded to the bias change- although performance remained superior at the obsolete bias locations (indicating preservation of the trained attentional strategies), performance also improved at or near newly biased locations (Fig. 6, difference images).

Changes in the distribution of V1 modulations, however, were more modest. Focal increases in the modulation of single positions may be seen, suggesting an increase in attentional resources being allocated to updated pattern, but modulation also remains undeniably strong at the formerly biased locations. Note, however, that the bias change did not impose an explicit penalty to detecting increments at the obsolete locations- subjects were given the same juice rewards for any successful increment detection, likely or unlikely. Thus, if the long-term training made attention to the obsolete locations more trivial, it might be advantageous for the animal to maintain old allocations while incorporating new information on the updated biases to increase overall task performance. Whether persistence of attention is beneficial in naturalistic stimuli remains uncertain, but in this task there was a real disadvantage from this mismatch in trained expectation versus current probabilities: Monkey F's sensitivity was significantly lower (-2%, $p < 0.05$,

binomial distribution), but a larger effect was seen in a significant reduction of the positive predictive value (PPV) of saccades in both animals (P: -4%, F: -6%, $p < 0.05$ in each). Thus both subjects' overall task performance was impaired by the change in contrast increment bias distribution.

While modulations were less adaptive to the new probability distribution, the correlation between positional modulations and positional sensitivity remained strong (Fig. 7; sensitivity: $r^2 = 0.57$, $p < 0.001$), while reaction time now strongly correlated with the new modulation pattern ($r^2 = 0.56$, $p < 0.001$). Together with the increase in false positives, we interpret the reaction time data as a change in both subjects' strategies as they learn the new task. Correlating modulations with behavior across both probability distributions, we find that over half of the positional variation in increment sensitivity and one-fifth of the variation in reaction time may be accounted for by the appropriate allocation of attention to the V1 population representing each stimulus (sensitivity: $r^2 = 0.558$, $p < .001$ reaction time: $r^2 = 0.219$, $p = 0.004$).

It is still possible that the overall correlation across both task conditions hinges on a fixed, underlying mechanism as discussed above. This is particularly concerning given the suggestion that the subjects may not have fully abandoned their older strategies. To explore this, we performed a final correlation analysis between the differences in behavior and attentional modulation across the two probability biases (Fig. 8). We found that increases in attentional modulation correlated with improvements in target sensitivity,

with an additional trend toward correlation with decreasing reaction time (sensitivity: $r^2 = 0.26$, $p=.03$; reaction time: $r^2 = 0.16$, $p=0.098$). This suggests that, regardless of any common factors that influence our subjects across both task conditions, the distribution of V1 attentional allocations predicts the ability to detect changes in retinotopically matched objects.

Discussion

Spatial Attention in Primary Visual Cortex

To date the highest resolution studies of task-based modulations within V1 rely upon electrophysiologic recordings. Even when using small stimuli, much like the single targets used in our study, these typically report modest effects: 0-10% increases in action potential firing rate are accompanied by non-specific changes in current source density or local field potential of the supragranular layers of V1 [9–11]. By contrast, strong modulations (>30% in many neurons) are observed using paradigms that require the animal to make perceptual judgments using information encoded by V1 (e.g. curve tracing [12] or detection of small target changes [13]), but these paradigms do not naturally restrict attention to address the limits of these modulations. In this study, we combine these two concepts, small stimuli and V1-level decision making, to produce a task which evokes strong ($\pm 30\text{-}40\%$) response modulations within V1 that influence task performance over a measurably limited spatial extent.

Our paradigm was engineered to require the involvement of V1. Even if the stimulus is small and optimal for V1, such as a bar or Gabor, any stimulus presented in isolation can be reliably detected by higher-level visual areas with larger receptive fields by integrating over the task-responsive and unresponsive regions of V1. There is no need to manipulate the visual representation as the finer V1 scale when modulation of higher areas with better connectivity to putative attention centers within prefrontal cortex [14] (e.g. the frontal eye fields) may be sufficient. As V1 does not receive direct [pre]frontal input [14], any attentional modulation of V1 from these regions must be multi-synaptic and therefore metabolically more expensive than modulation of higher level areas with a shorter network distance. Moreover, as V1 contains the lowest level visual cortical representations it also contains information closer to the ground truth of physical reality. If the attention system can accomplish target selection without perturbing this early map, it will allow one to preserve this representation while also performing the task at hand. This may serve to prevent inattention blindness [15] (which is known to impact early visual area MT [16]) to important low-level stimuli such as brief motion pulses which could signal danger. For these reasons, there is utility in limiting attentional modulations of V1 unless the task is spatially complex [9].

Our task, however, can not be solved simply by increasing the signal gain over the entire array, as might occur if only higher visual areas with larger receptive fields were modulated. Importantly, both subjects found it impossible to reliably detect contrast

increments in the singleton stimuli at the same threshold that increments were detected in the array. Our task was only possible if subjects we able to to notice differential contrasts between adjacent stimuli. This forced the monkeys to make perceptual judgments over fine partitions of visual space on the order of V1 neural receptive fields. Note that this task requirement arose naturally from the structure of the stimulus array and was not explicitly instructed- the comparison of neighboring-element contrasts appears to be a natural strategy for both animals.

In contrast it is well-established that imaging studies of attention in V1, particularly fMRI, tend to show large modulations of V1 activity- up to 100% or more, on the order of the underlying visual signal. It has been proposed that this is due to the ability of fMRI to integrate a weak signal over the entire neural population contributing to the voxel's BOLD response (>1 million neurons) [17]. Like BOLD, the AF signal we measured in this study integrates physiologic responses from a population of neural and non-neural cells. While we can not rule out the possibility that AF imaging is similarly sensitive to subthreshold modulations, note that the scale of this averaging operation is much smaller in our imaging than in typical fMRI studies. First, by analyzing early time periods, we may rule out the influence of any hemodynamic signal including the pooling of responses within large venules [17,18]. Second, the individual pixels in our preparation reflect an area of approximately $4E-4 \text{ mm}^2$, sampling the mitochondrial response from only hundreds of neurons. If the responsitivity of imaging signals such as BOLD and AF to attentional

modulations in V1 relied on a simple average of the modulations of many neurons, we would expect our modulations measured by AF to be much closer to the responses seen in single-unit studies. Given that we see modulations as strong as 40% at single positions, this is clearly not the case.

It is also unlikely that the AF signal is representing non-visual and non-attentional information in our task. All modulations reported here are time-locked to the visual stimulation and are base-line subtracted- the signal due to non-neuronal background physiology is removed from our images. Moreover, as action-potential related changes account for the majority of the brain's energy consumption [19], we expect the mitochondrial AF signal to closely approximate neural processing on short, stimulus-evoked time frames. Our estimates of the attention component of our signal are not corrupted either by visual information or by modulations due to task performance [1], as we only measure attention as a difference between two task conditions with identical task rhythm and visual stimulation.

Rather, we suspect that attentional modulations may readily reach V1, but that this process only exerts a strong effect when required by the task. The addition of this task requirement poses a non-trivial challenge to the simple model of attentional targeting that is proposed in this thesis: regardless of whether the task is easy or difficult, of whether stimuli are presented singly or hidden within an array, the most task-appropriate cell in the brain would remain the same V1 neuron whose receptive field matches the stimulus.

Why, then, might attentional targeting be a function of task demands as well as the nature of the attended stimulus?

A substantial clue may arise from the mismatch between the target locations and their attentional modulations: in both animals, several continuous elements showed attentional modulations and a perfect selection of the bias targets appeared impossible, but none-the-less modulations were grossly targetable to at least one half of the array.

Assuming the magnification factor of Monkey F and P's underlying V1 retinotopy is similar, this suggests both that attentional modulations may be precise to within 0.5-1 degree of visual space, but no more precise than 0.3-0.4 degrees (the interstimulus spacing of each animal). In cortical space, this represents precision at the scale of 2-3 mm but imprecision under 1mm. In agreement with these values, corticocortical feedback axons from V2 branch along 1-4 mm of the V1 cortical surface.

In postulating that the precision of V2-V1 feedback is a hard limit to the attentional selection of visual space, we imply that these feedback processes carry attentional information. V2 provides equal or greater input to V1 than does the lateral geniculate nucleus [20]- while this feedback has long been known to influence non-attentive processes such as contour end stopping and surround suppression [7], we imply that these same circuits also carry conscious attentional influences which may provide equally strong influences to V1 processing. Moreover, we provide evidence that attentional

modulations must reach V1 by traveling through the visual hierarchy and that other feedback projections to V1 do not provide more precise spatial information.

Attentional modulations of V1 variably impact performance

We demonstrate a strong correlation between response modulations in V1 and task performance on the scale of fractions of a visual degree, and show that these modulations can support trained (Fig. 5) and untrained (Fig. 7) probability patterns. Moreover, V1 modulations facilitate the change between patterns (Equation 1). This suggests that our observed modulations within V1 are not simply the result of longitudinal training but rather do respond flexibly to changing task demands.

However, the nature of the behavioral improvements associated with V1 response modulations appear to be a function of other variables in the animal's global state. With the original, highly trained position bias, both subjects were less likely to make a false positive saccade. However, when exposed to an alternative bias distribution, the sudden task uncertainty causes an increase tendency for invalid saccades in both animals. At the same time we observed a strong correlation between positional reaction time and attentional modulation when attending to the alternative but not to the original bias. We interpret this as the animals changing the speed-accuracy trade off of their V1 readout task uncertainty increases and they must learn the new bias distribution. This may occur as a result of coincident modulation of other visual areas, or through changes in how both

animals convert continuous visual information into a binary perceptual decision [21].

Thus the effects of V1 attentional modulations on task performance are not constant, but rather change as a function of greater task demand. This provides a novel route for further flexibility within the attention system.

	Monkey F				Monkey P				Overall	
	Original		Alternate		Original		Alternate		Bias	SS
	Bias	SS	Bias	SS	Bias	SS	Bias	SS		
Attention	-0.66	-0.101	-	-0.034	-0.36	0.062	-0.31	-0.067	-0.41	-0.043
(p)	4.4E-4	<1E-6	-	8E-4	0.085	0.014	0.14	0.017	7E-4	<1E-6
Sensitivity	0.17	-0.080	-	-0.071	0.34	-0.0093	-0.13	-0.057	0.013	-0.060
(p)	0.15	2.5E-4	-	<1E-6	0.0014	0.28	0.080	6E-6	0.39	<1E-6
Rxn Time	26.2	6.44	-	3.28	13.1	6.45	22.1	7.22	10.57	5.42
(p)	0.13	0.035	-	0.012	0.15	2.5E-4	0.029	3E-6	0.06	<1E-6

Regression beta values for controlled variables in the behavior versus positional modulation partial correlation analysis. Bias term not included in Monkey F's Alternate bias because it was uniform. The effect of the probability bias on target sensitivity was varied, likely reflecting different strategies between original and alternative biases. The bias otherwise consistently negatively impacted both attentional modulations and reaction times. Surround suppression almost uniformly impairs both attention and task behavior across data subsets. Bias, the probability distribution of increments; SS, surround suppression.

End Notes

Acknowledgements This work was supported by.

Author Contributions SGW implemented the task design, acquired the data and performed the data analysis. GMG and SGW worked together on experimental design, animal surgeries, data analysis, and manuscript preparation.

Figure Legends

Figure ?? | Attention to Fine Objects. **a** Animals fixate at a center point while a 3x3 array of drifting Gabors is presented in each hemifield. At a random time, one of the 18 Gabor targets will briefly increase in contrast. Subjects report detection of this increment by a saccade to the appropriate array. **b** The individual Gabors are approximately 50% larger than the expected receptive field size of V1 neurons at the stimulated location. When viewed at arms length (60 cm), this panel shows the location of the stimulus array to scale for each animal. Monkey F (P) refers to the subject with the more foveal (peripheral) stimulus array. **c** Each trial block (20-50 trials), subjects are cued (black circle) as to whether the increment is more likely (96%) to occur in or outside of the imaged region of V1. The cue is communicated via instruction trials (see text). Subjects were trained over several months that two locations (one foveal, pink, and one peripheral, cyan) are eight times as likely to increment. **d** Representative behavioral data from one animal. Peripheral increments were easier to detect, but with training performance increased at the foveal target.

Figure ?? | Differential activity to individual Gabors. In a separate task, each of the 9 Gabor targets was presented individually. The distribution of optical signal from V1 reliably changed as a function of Gabor location, consistent with the known retinotopy of V1. **a** Timeseries of averaged optical signal from Monkey P when only the foveal (top row)

or peripheral (middle row) target is presented. Bottom show shows a difference image between the top rows. Although the target centers are separated by only 1.13° in visual space, we may localize activity from one or the other target. The other 7 positions were also mapped with equal precision (not shown). **b** In both animals, differential activity as a function of stimulus location appears immediately after stimulus onset. Green highlight indicates the time frame from which the position-tuning of each pixel is estimated in future analysis. This time matches the time of observed attentional modulations (Fig 3).

Figure ?? | Gross attentional dynamics. Line traces show the average optical signal from a region of interest integrating activity from all 9 positions while subjects direct attention toward (red) or away from (blue) the imaged region of V1. In this and all figures demonstrating attentional differences, only images collected prior to a saccade or contrast increment are included. Early in the trial, attention increases activity across V1 of both animals. Late in the trial, the early mitochondrial signal from Monkey P is washed out by a negative signal of known hemodynamic origin. No such confounding signal was observed in Monkey F. To avoid ambiguity about the origin and sign of the relevant signal, in later figures we analyze attentional activity only from the early trial period indicated in green.

Figure ?? | Attentional modulation of individual targets.. We reconstructed the distribution of attentional modulations as a linear combination (see text) of the activity patterns observed when the individual stimuli were presented (Figure 2). Positive (negative) "positional modulations" imply enhancement (suppression) of the individual

target's V1 representation. The colored background on the modulation distributions indicates the magnitude of a coincident global modulation that enhances or suppresses all stimulus representations. For both animals, neither the reconstructed attention distribution nor task performance perfectly match the probability schedule, however biases toward the cued sides of the array are evident. Scale bars show the extent of the stimulus array in retinotopic coordinates (black) as well as across real cortical space (green) where available.

Figure ?? | Attention targeted to individual targets.. **a** The partial correlation between reconstructed positional attention modulations and stimulus sensitivity (controlling for each variables individual correlation with the probability bias) is high, strongly implying that attentional modulations at a given target's V1 representation enhances detection of changes at that target location. **b** A trend toward the same is seen in the correlation between attention and reaction time.

Figure ?? | Alternative Probability Schedules - Two-dimensional Distribution.. A abruptly, the long-term bias in target probability as a function of position was changed for each animal (left column). Monkey P was trained on a rotated probability distribution, where Monkey F was trained on a uniform distribution. Both animals changed their behavior (right) and attentional allocations (left) to accommodate the change, however performance remains imperfect. Top row for each animal shows the new distributions for the updated bias, and the bottom row shows a difference in performance between the two

bias distributions. Format is otherwise the same as Figure 4. Both animals only partially adopted the new distribution and each had a tendency to maintain attention and improved performance at the obsolete bias locations.

Figure ?? | Alternative Probability Schedules - Behavior Partial Correlation.. Under the new probability schedule (Figure 6), attentional allocations across V1 remain correlated with sensitivity (A) and with reaction time (B). The overall correlations between attention and sensitivity, including both the original and altered probability schedule across both animals (not shown), strongly suggest that these modulations are involved in stimulus perception (overall sensitivity: $r^2 = 0.558$, $p < .001$; overall reaction time: $r^2 = 0.219$, $p = 0.004$).

Figure ?? | Difference Between Probability Schedules - Behavior Partial Correlation.. As the subjects switch from the original to the alternative bias distribution, their behavior and attentional modulations change as a function of stimulus position. These changes are correlated. (A) The change in increment sensitivity correlates with the change in attention between the two bias distributions. (B) The change in reaction time shows a trend toward correlation with attentional modulations.

Methods

Subjects

Two adult male rhesus macaques (*Macaca mulatta*, 13.5 and 9.8 kg) were enrolled in this study. The two subjects were fluid restricted and trained using positive reinforcement to perform a change detection task in return for a fluid reward (Gatorade). All experimental procedures were approved by the Institutional Animal Care and Use Committee of the University of Minnesota, an Association for Assessment and Accreditation of Laboratory Animal Care International accredited organization. Both subjects were attended daily by professional veterinary staff and had daily access to food, activity, and audiovisual enrichment.

Behavioral Paradigm and Analysis

Two macaques (Monkey F and Monkey P) performed the change-detection task outlined in Figure ???. Subjects maintained fixation within 0.5° at a 0.125° white fixation dot for a long (variably 500-2000 ms, uniform distribution) prestimulus period after which two 3x3 arrays of small (F: 0.3°, P: 0.4° diameter) Gabor appear symmetrically on screen, one each in the left and right visual hemifields. The array elements are positioned such that the middle column is isopolar along the vector from the fixation point to the center of the array- the remaining 6 Gabor are distributed in neighboring columns parallel to the

isopolar column. The Gabors are high contrast (F: 35%, P: 20%) and continuously drift (4 Hz) in order to strongly activate V1 neurons. Gabor orientation and drift direction are uniform across each array, but are balanced between stimulus arrays such that net motion along the horizontal axis is zero. The spatial frequency of each element is appropriately scaled such that one full cycle is always present. Visual stimuli were generated using custom software, and presented on a CRT monitor with 85 Hz refresh rate positioned 495 mm from the subject. Subject eye position was continuously monitored with a monocular iViewX infrared camera and analyzed on-line with the same custom software. On-line deviations of 0.9-1.4 degrees from fixation were permitted; this lax window was required for subjects to maintain fixation for 8 seconds per trial. Larger deviations caused trials to immediately abort with no reward; this typically occurred only during saccades or eye blinks. During off-line analysis, only attention data collected from the time period between the onset of the stimulus array and the first fixation deviation greater than 0.5 degrees are analyzed. Typically, this excludes a large microsaccade.

At a random time (400-6150 ms, exponential distribution with uniform hazard function), one of the 18 Gabor elements briefly (94 ms) increased contrast (P: to 32%, F: to 52%). The increments were difficult to detect and the task required the subject's constant vigilance. For both subjects, task performance was well distributed between true positive, false positive, and false negatives. The overall hit rate to detect targets was 62.5% for Monkey F and 81% for Monkey P. The predictive value of a saccade was 52% for F and 70% for P. On

10% of trials, no contrast increment occurred and subjects were rewarded for maintaining fixation. Both subjects performed the task at their maximum tolerated difficulty (the smallest tolerated contrast increment) in order to force the greatest possible amount of attention to the targets- adjustments of 1-2% to the contrast increment caused a precipitous decrease in overall behavioral performance in both animals (observed during on-line analysis but not shown).

If subjects reported detection of the increment via a saccade to the target array, a juice reward was administered along with a positive sound cue. If subjects broke fixation from the central dot for any other reason, the trial was aborted with no reward and a negative sound cue. At this task difficulty, both animals exhibited a strong tendency to make a false positive response early in the trial (consistent with a high-uncertainty, guess-based strategy). To reduce this tendency without sacrificing the visual difficulty (attentional demand) of the task, we made several manipulations to the reward and intertrial schedule. The juice reward administered on a given trial was non-random and increased exponentially with successive true positive or true negative responses, up to a maximum of one second of continuous fluid administration. This reduced the expected value of continuous guessing, as randomly correct performance would usually administer only the smallest reward. Moreover, when a false positive response was recorded, the next trial was delayed by a period of time equal to the time remaining in the trial. This provided a maximal punishment time-out for early guesses (to discourage the animal from rapidly

cycling through trial attempts) but only minimally punished a putatively effortful false positive that occurred later in the trial. While the effect of these performance manipulations was not carefully measured, the end result was that both subjects maintained effort in spite of a very difficult task for which a juice reward was administered infrequently relative to a more typical macaque behavioral paradigm (on some days, including fixation breaks, <30% of trials resulted in a juice reward). Physiologic fluid requirements for each subject were met daily and exceeded weekly via supplementation with unflavored water as necessary.

To manipulate visuospatial attention, the probability that the increment would occur at a given target position was non-uniformly distributed. The subjects were given two different cues to direct attention to a subset of the stimulus elements. First, in each trial block (20-25 trials), the increment would occur in either the left or the right hemifield on 96% of trials. This left/right cue was explicitly given to the subjects by a series of 4-5 instruction trials preceding each block during which only the likely hemifield was stimulated. A second cue was given to the animals in the form of their training history. For months prior to imaging data acquisition, the same two target locations (one on the foveal and one on the peripheral side of the array) were eight times more likely to increment. Prior to imaging, both animals demonstrated a behavioral preference for detecting increments at one or both of these locations. The same locations are biased during training and image acquisition, except that in the final data collection sessions for each subject the

intra-array locational bias was abruptly changed. In Monkey F, the bias was removed completely and replaced with a uniform probability distribution. In Monkey P the bias was rotated such that the opposite corners of the array were now eight times more likely to increment. The new bias was then held constant over several imaging sessions.

We estimated the subjects' overall task performance by fitting both increment sensitivity (the percentage of detected contrast increments) and saccade positive predictive value (PPV, the percentage of saccades that correctly identified an increment) over all positions to a binomial distribution. To estimate detection performance at each position, we only considered the sensitivity to each position's increments as we could not reliably determine at which position an increment was falsely perceived during false positive saccades. When plotting these data linearly, we collapsed the two-dimensional array of positions into a one-dimensional representation by averaging all positions that were equidistant from the foveal and peripheral bias location (the vertical axis in Figure ??C).

Each subject also performed a similar task during 'position tuning' sessions in which only a single Gabor was presented, of the same size as and at one position of those in the 3x3 array experiment. The purpose of this was to record the visually evoked activity across V1 attributable to each individual stimulus element. During these position tuning measurement trials, the subjects detected a larger contrast increment which always occurred within the single Gabor; both subjects were unable to detect the original contrast increment within a singleton Gabor and required this easier detection.

In a variant of the position tuning task, subjects detected singleton stimulus contrast increments over a variety of stimulus radii and base contrasts. Imaging data from these trials was used to verify the visual response of the chamber but was not otherwise utilized during subsequent analyses.

Immediately after the chamber implantation and prior to position tuning and task performance, both animals also participated in conventional retinotopic mapping of the chamber. Estimated retinotopy from these methods was used to place the stimulus array in an appropriate location within the visual field, but no analysis of task performance or attentional modulation relies on these traditional retinotopic measurements- all correlation between task signals and individual stimulus positions utilizes the position tuning measurements described above.

Image Acquisition

Utilizing sterile surgical technique while subjects were under general anesthesia, we made a craniotomy and durotomy over V1 of each subject. V1 was identified anatomically by visualization of the operculum of V1 (ensuring that the exposed region of V1 is not near the lunate sulcus and V2/V4) and by cranial landmarks. To maintain patency of the craniotomy and durotomy, a biocompatible polymer (polyethyl ether ketone) imaging chamber and transparent artificial dura were placed over V1. The artificial dura was stabilized between behavioral sessions with a rigid chamber insert. Prior to each imaging

session, hygienic cleaning of the skin, exposed implant surface, and the dura margin was performed. To reduce physiologic movement artifacts and glare, the subdural space of each animal was flushed with sterile normal saline via tubing inserted through the artificial dura, and the imaging chamber was filled with sterile normal saline.

After recovery from surgery, both subjects performed the task seated upright and comfortably while V1 was imaged with a Cascade 512b charge-coupled device camera. The camera was suspended over the animal's exposed V1 and held rigidly to the behavioral apparatus. Focus was manually adjusted daily onto a plane 0.5-1.0 mm below the surface of the brain. Differences in the field of view of the camera between different behavioral sessions (due to small changes in the position of the subjects, their behavior chairs, and the camera) were tolerated and corrected with off-line image registration (see below). The camera acquired a 256x256 pixel image spanning $\approx 8 \times 8$ mm of the cortical surface five times per second. The implied resolution of these images is thus $23.4 \times 23.4 \mu\text{m}/\text{pixel}$. The chamber was illuminated with blue light (415-485 nm band-pass Chroma D455/70x filter); with Monkey F we used a DC tungsten light source and with Monkey P we used a light-emitting diode to reduce illumination noise. In a set of control experiments targeting the hemodynamic intrinsic signal instead of the AF signal, the chamber was illuminated with red light. Light entering the camera was again filtered (520 nm long-pass Chroma E515LPv2 filter) before pixel binning, on-chip multiplicative gain (15-20x amplification), and digitization to generate a monochromic, unsigned 16 bit

integer image. The same custom software used to present visual stimuli also collected these images, tagged each image with a time stamp relative to behavioral task events, and saved the images to disk for off-line analysis- on-line analysis of images was limited to ensuring appropriate camera positioning and focus.

Off-line Image Processing

Each image was converted from a RAW bytestream to MATLAB 16-bit arrays using custom conversion software. Each image was reoriented to reflect the true left/right and up/down axes, and hardware-level image acquisition errors (e.g. image tears) were detected and eliminated using custom MATLAB code. Within each behavioral trial, motion correction between images was performed by selecting the first image acquired after stimulus onset and then translating all other images from the trial such that the mutual information between all images was maximized. Across behavioral trials, differences in the position and angle of the camera were corrected for by a 6 degree of freedom affine registration between the two images series. Intratrial motion correction was automated using gradient descent methods, but intertrial motion correction required substantial manual intervention. Errors due to manual imprecision were minimized by oversampling the number of registration points between images using 9 instead of the minimum 3 control points.

Because the animals are seated up-right and the chamber protrudes from the parietal bone at an angle, the gravitationally determined water line is not normal to the brain surface and a small hyperintense glare is present from the illuminator in nearly all images from the anterior portion of the chamber. Hyper- and hypointensities are also present near the edges of the artificial dura. Such abnormal regions of each image were liberally masked by thresholding each image and then further removing a 5-pixel edge from the edge of the thresholded image, and the motion-corrected images from each trial were then converted to units of percent-change by dividing each trial's image series by the respective trial's first post-stimulus image. The image series from each trial was aligned to the onset of visual stimulation, and images occurring before fixation or after either a fixation break/saccade or after a contrast increment were discarded. These aligned image series were averaged for each stimulus condition.

Individual Position Tuning

Once the approximate retinotopic location of V1 within each imaging chamber was found using standard methods [?], we measured the pattern of activity evoked across the chamber when each individual stimulus element of the array was presented in isolation.

In Monkey P, the individual stimuli evoked a clear and reliable distribution of V1 activity across adjacent locations that matched the known topology of the retinotopic map.

However, the evoked activity from individual stimuli typically demonstrated a negative

response that lasted several seconds- this is very typical of the known time course and signal directionality of hemodynamic signals that are known to potentially interfere with AF signals [4]. In relating position tuning from Monkey P to his attentional modulations (which were positively signed), we inverted the sign of his position signals such that estimates of stimulus position were positive for the receptive field centers of each element.

In Monkey F, we mapped position tuning preferences with smaller stimuli, at a higher contrast, at a more foveal location, and through a layer of neomembrane (a thickening of the remaining layers of dura that occurs naturally as the imaging chamber ages). The net result of these differences is that each individual element evoked a wide-spread activation pattern including the entire imaging chamber. None-the-less, this pattern was distinct for each position, with centers-of-mass that crudely aligned with retinotopic topology. Separable regions of activation for each position emerge in Monkey F's position tuning estimates over the same timecourse as seen in Monkey P. Thus while we could not create a 1-to-1 mapping from V1 pixels to stimulus positions, we could still construct for each pixel a position tuning curve. Using these tuning curves, we can use multi-pixel pattern analyses to decompose primary task activity across the chamber into a discrete prediction of activity within the neural representation of each stimulus position (see below).

Informed by these position tuning estimates, we manually selected a region of interest within each chamber that included responsive pixels for all nine stimulus positions plus surrounding cortex. This ROI included 39,414 pixels (21.6 mm^2) from Monkey F and

16,698 pixels (9.17 mm^2) from Monkey P. The larger ROI of Monkey F includes the larger extent of his position tuning evoked activity. Differences in the images area between animals are controlled by performing pixel-wise analyses separately for each animal before combining data.

Analysis of Attentional Modulations

We observed both a substantial visual-evoked and a non-visual, non-attentive response from V1 under all task conditions. Monkeys performing tasks with a similar structure (cycling between intertrial, stimulus, and response epochs) have shown a large intrinsic signal change in V1 that is correlated with the dynamics of the task independent of visual stimulus [22]. To control for visual and non-visual signals, in our study we exclusively study attentional modulations as defined by the difference between images collected while animals attend the stimulus in the hemifield contralateral to the imaged hemisphere (“attend in”) and images collected in the opposite cue condition (“attend out”). We discarded trials which were shorter than 1 second, as they did not contribute sufficiently to our targeted attention period (600-1600 ms post-stimulus).

By averaging hundreds of trials of each type together (Monkey P, 847 Attend In trials, 881 Attend Out trials; Monkey F, 502 Attend In trials, 503 Attend Out trials), we obtained an estimation of the distribution of attentional modulations across the cortical surface. After finding that in both subjects the sign of the attentional modulation is positive from

600-1600 ms after stimulus onset, we averaged data from that time interval to generate a mean attention modulation and mean single position evoked activities. Use of data from the early trial period also avoids conflict between mitochondrial and vascular sources of optical signal [4]. We decomposed this mean attention into an estimate of activity at distinct positions by performing a multiple linear regression of the attention map against the activity patterns evoked by each individual position. That is, we modeled the attentional map as a linear sum of the individual positions' visual activity maps

$$MeanAttentionalModulation = \sum_{pos=1}^9 \beta_{pos} \times MeanSinglePositionEvokedActivity_{pos} + C \quad (1)$$

where the beta values are computed by standard linear regression. We use these beta values as measurements of "Positional Modulation." This regression analysis has one crucial advantage over a region-of-interest based analysis, in that it naturally accommodates pixels that are on the border of the V1 representation of two positions and so respond to both stimulus elements. Due to the point spread function of the AF signal [4], the measured representations may overlap even though the stimuli do not overlap in visual space.

Both attentional and positional activity terms in 1 are vectors containing data from all pixels in the visually responsive region of interest within each animal's V1. This regression

analysis considers attentional modulations toward a given stimulus as an all-or-nothing linear change including all images pixels in the center and surround fields of each position's visually evoked response. Non-linearities may be implied by the map of residual attentional modulations which are not accounted for by this model, but such residuals are not further explored in this report due to the inferior retinotopy of Monkey F.

To improve the overlap between position tuning and attentional modulation images, we smoothed all composite images by a $116 \mu m$ Gaussian kernel. The activity maps for each position were not normalized- thus each beta may accurately be interpreted as the proportion of that position's activity that is present within the attention map. For example, a beta value of 0.2 would imply an attentional modulation that is 20% of the magnitude of the position's original evoked activity.

To compare V1 physiology with subject behavior, we computed partial correlations between positional attention and sensitivity that remove the influence of the probability distribution of the stimuli from both the positional modulations and the behavioral distributions. This allows us to explore whether variation in attentional modulations correlate with variations in task behavior without confounding this relationship with the increased task performance at high probability locations. The partial correlation is computed as the Pearson's R correlation coefficient between the residuals that remain after the probability distribution is independently regressed out from the positional modulations and behavioral distributions. For this analysis, due to the sparse sampling of

behavior at the unbiased locations we used sensitivity computed from all time points. Our major conclusion, that positional attention is correlated with contrast increment sensitivity ($r_{partial}=0.414, p<0.001$, Figure ??, still holds when sensitivity is restricted to stimuli presented during the analyzed time period with timing adjusted for the delayed AF impulse response function ($r_{partial} = 0.164, p = 0.014$). The partial correlation for reaction time is reduced to a trend by restricting analysis to early correct trials ($r_{partial} = 0.076, p = 0.108$).

In Monkey F, the same factors that decreased the quality of our position tuning (small, closely packed, high contrast stimuli, larger fixation variance) also may account for increased surround suppression within his stimulus sensitivity measurements. This is readily observable as higher sensitivity to detect increments at the corners of the stimulus array (the least crowded locations) and reaches statistical thresholds for significance in Monkey F but not in Monkey P (Table chapter:imaging::table:betavalues). For Monkey F, we also removed the influence of surround suppression in his partial correlation analyses. This improves the relationship between behavior and positional modulations in Monkey F, but outcome of our correlation analyses over the full data set are robust to the inclusion or exclusion of the surround suppression term in either animal.

References

- [1] Cardoso, M. M. B., Sirotin, Y. B., Lima, B., Glushenkova, E., and Das, A. *Nature Neuroscience* **15**(9), 1298–1306 (2012).
- [2] Van Essen, D. C., Newsome, W. T., and Maunsell, J. H. *Vision Res* **24**(5), 429–448 (1984).
- [3] Carrasco, M. *Vision Research* **51**(13), 1484–1525 7 (2011).
- [4] Sirotin, Y. B. and Das, A. *Front Neuroenergetics* **2**, 6 (2010).
- [5] Kalatsky, V. A. and Stryker, M. P. *Neuron* **38**(4), 529–545 5 (2003).
- [6] Simoncelli, E. P. and Schwartz, O. *Advances in Neural Information Processing Systems* **11**, 153–159 (1998).
- [7] Nassi, J. J., Lomber, S. G., and Born, R. T. *The Journal of neuroscience : the official journal of the Society for Neuroscience* **33**(19), 8504–8517 (2013).
- [8] Chicherov, V., Plomp, G., and Herzog, M. H. *NeuroImage* **2** (2014).
- [9] Motter, B. C. *J Neurophysiol* **70**(3), 909–919 (1993).
- [10] Mehta, A. D., Ulbert, I., and Schroeder, C. E. *Cerebral Cortex* **10**(4), 343–358 4 (2000).
- [11] Moran, J. and Desimone, R. *Science* **229**(4715), 782–784 (1985).
- [12] Roelfsema, P. R., Lamme, V. A., and Spekreijse, H. *Nature* **395**(6700), 376–381 (1998).
- [13] McAdams, C. J. and Reid, R. C. *J Neurosci* **25**(47), 11023–11033 (2005).
- [14] Felleman, D. J. and Van Essen, D. C. *Cereb Cortex* **1**(1), 1–47 (1991).
- [15] Simons, D. J. and Chabris, C. F. *Perception* **28**(9), 1059–1074 (1999).
- [16] Harrison, I. T., Weiner, K. F., and Ghose, G. M. *J Neurosci* **33**(19), 8396–8410 5 (2013).
- [17] Boynton, G. M. *J Vis* **11**(5), 12 (2011).

- [18] Turner, R. *NeuroImage* **16**, 1062–1067 (2002).
- [19] Attwell, D. and Laughlin, S. B. *Journal of cerebral blood flow and metabolism : official journal of the International Society of Cerebral Blood Flow and Metabolism* **21**, 1133–1145 (2001).
- [20] Muckli, L. and Petro, L. S. *Current Opinion in Neurobiology* **23**(2), 195–201 (2013).
- [21] Bogacz, R., Brown, E., Moehlis, J., Holmes, P., and Cohen, J. D. *Psychol Rev* **113**(4), 700–765 10 (2006).
- [22] Lima, B., Cardoso, M. M. B., Sirotin, Y. B., and Das, A. *Journal of Neuroscience* **34**(42), 13878–13891 10 (2014).

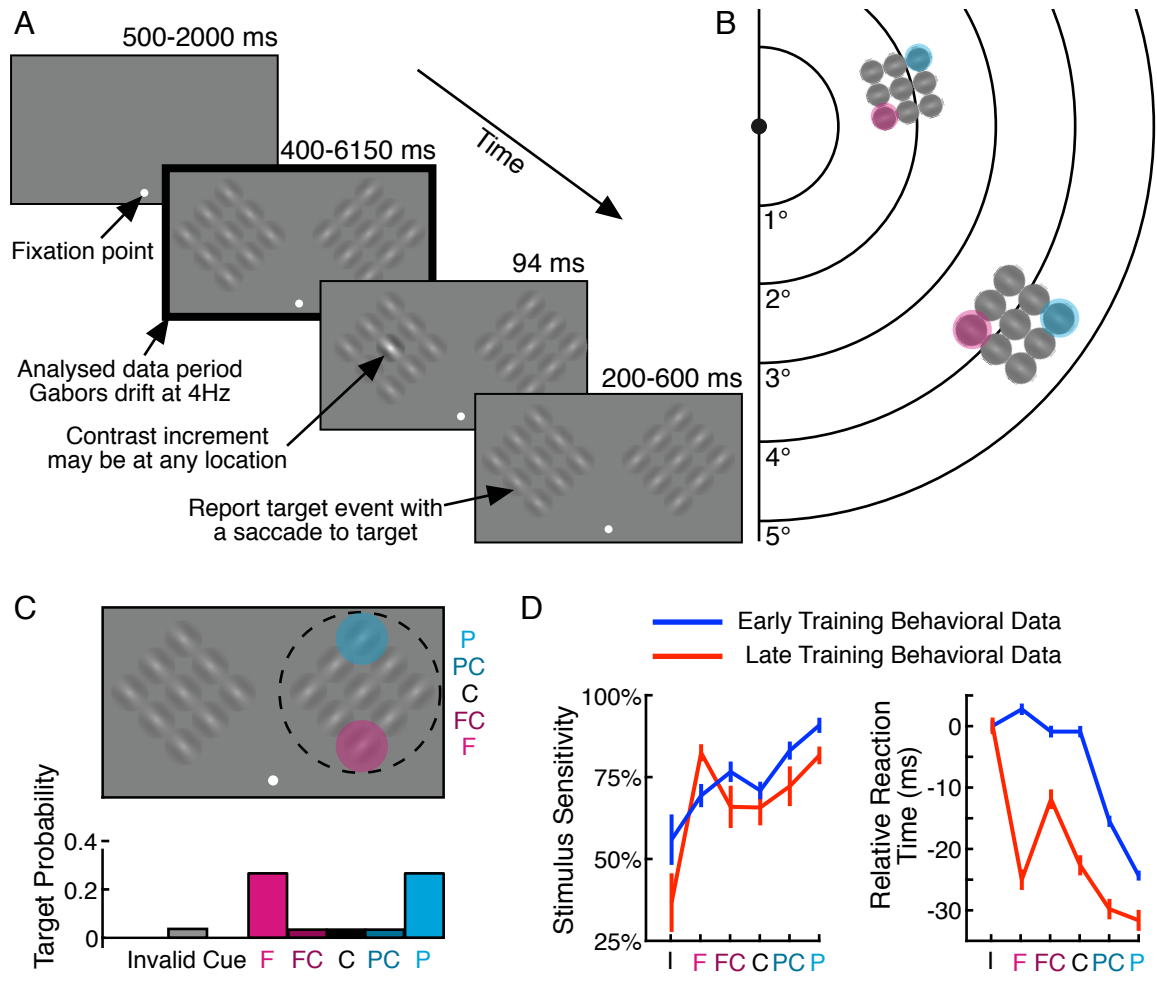


Figure 1

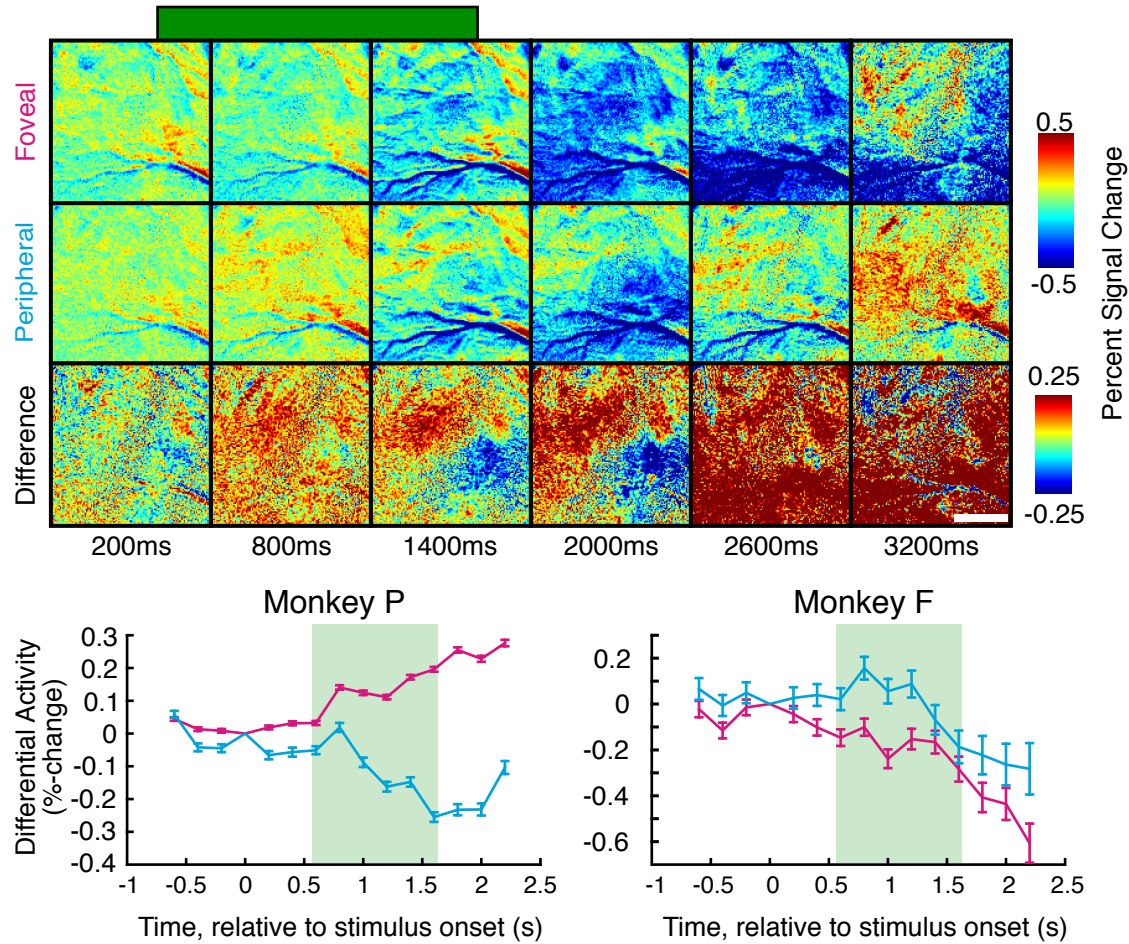


Figure 2

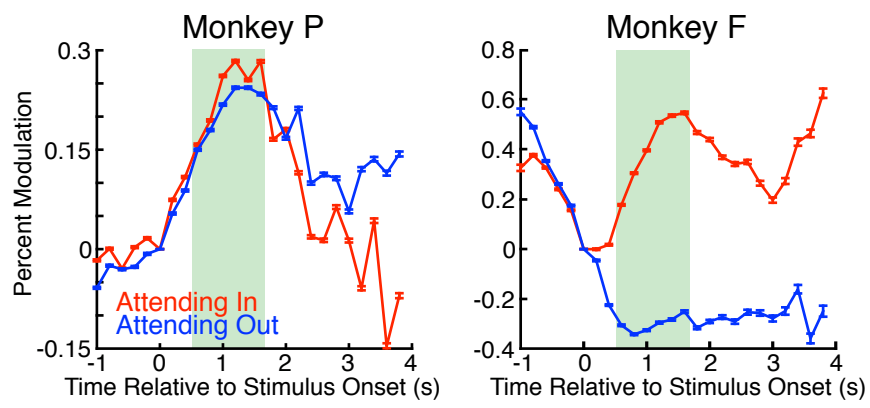


Figure 3

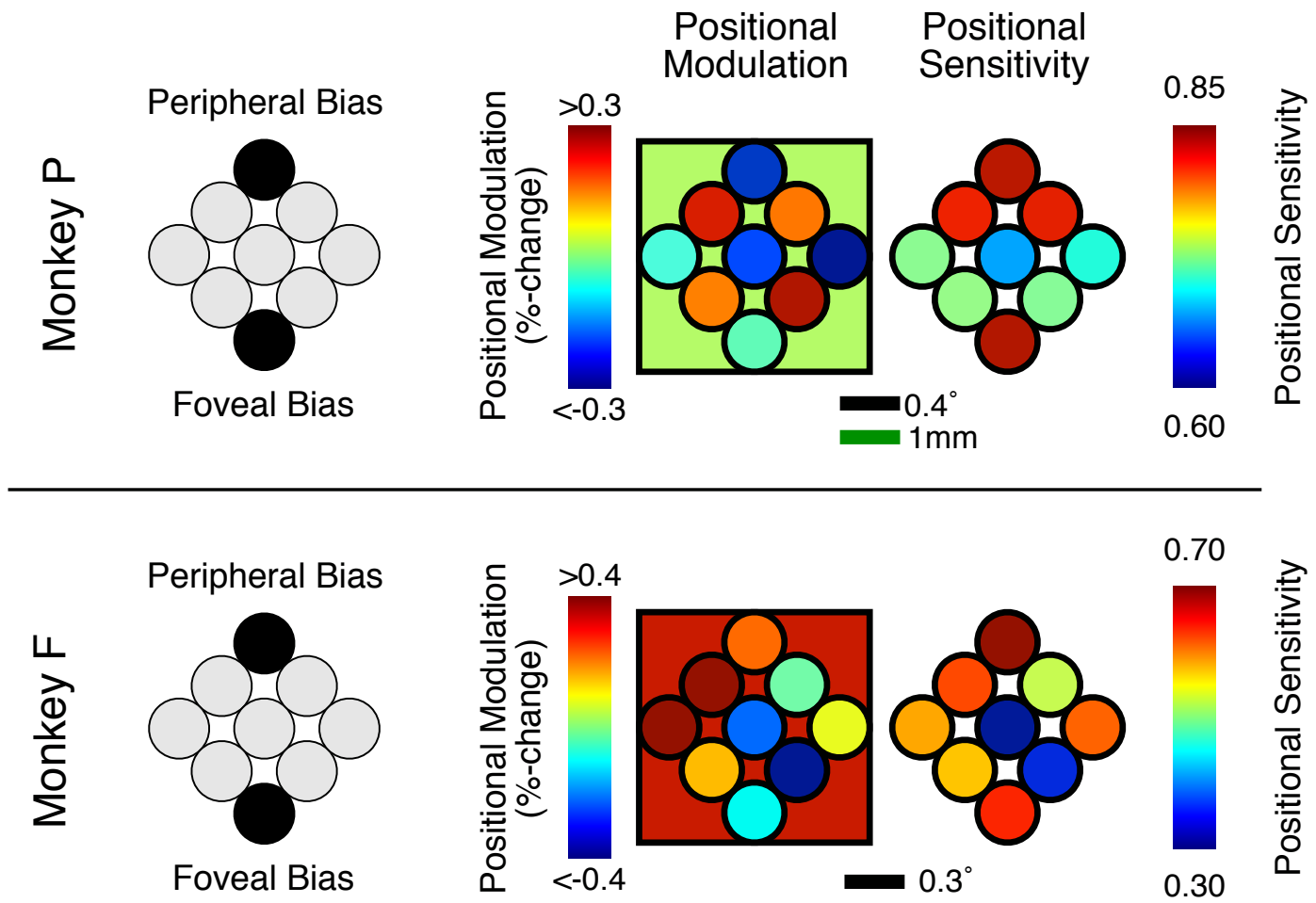


Figure 4

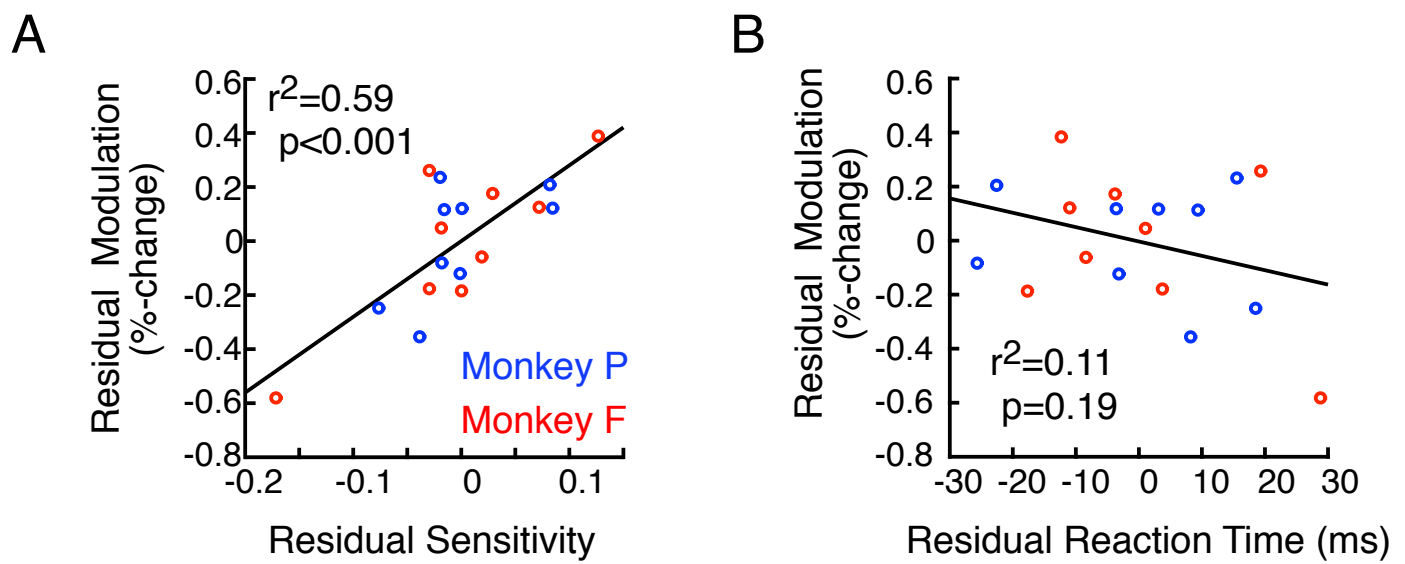


Figure 5

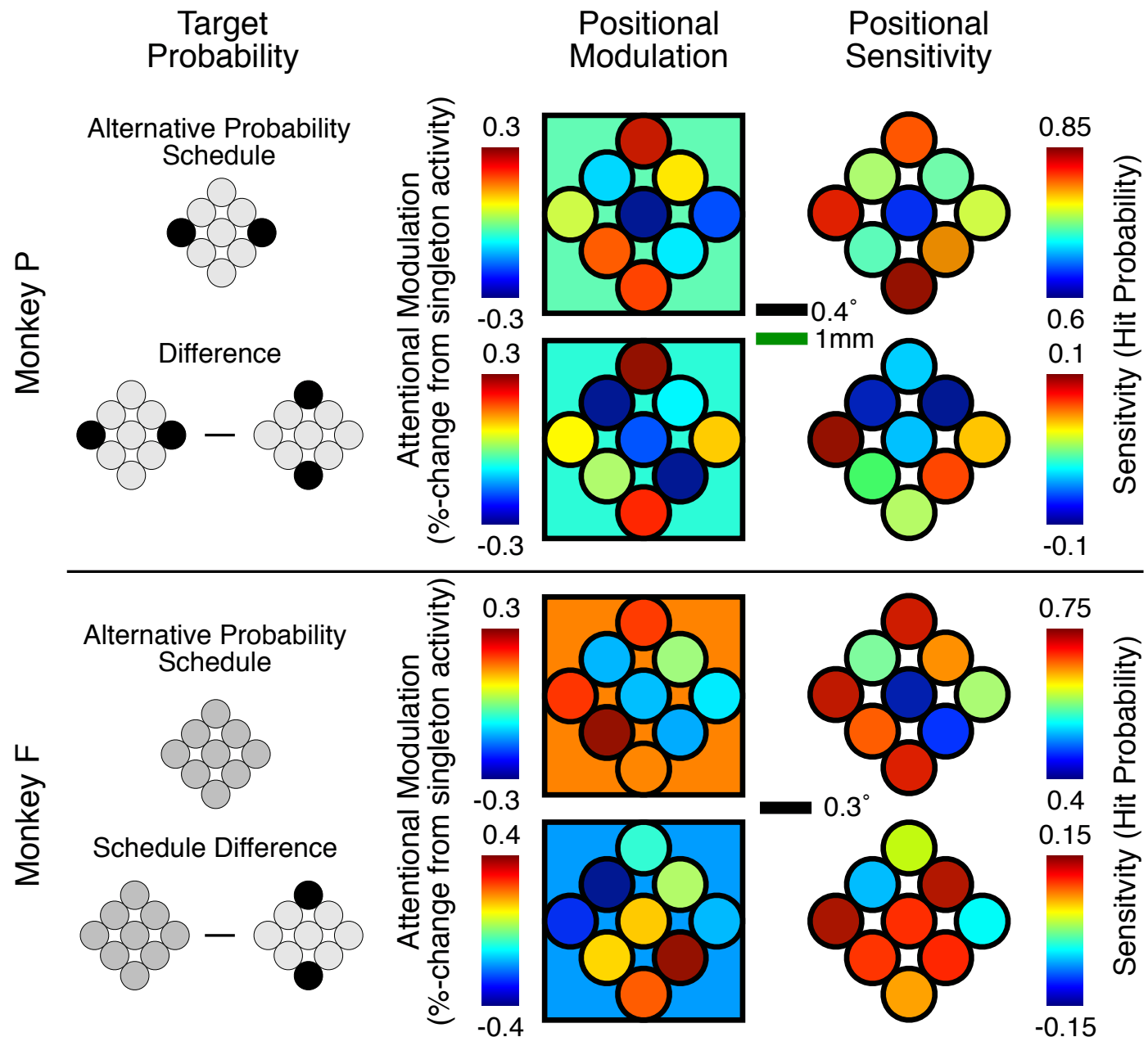


Figure 6

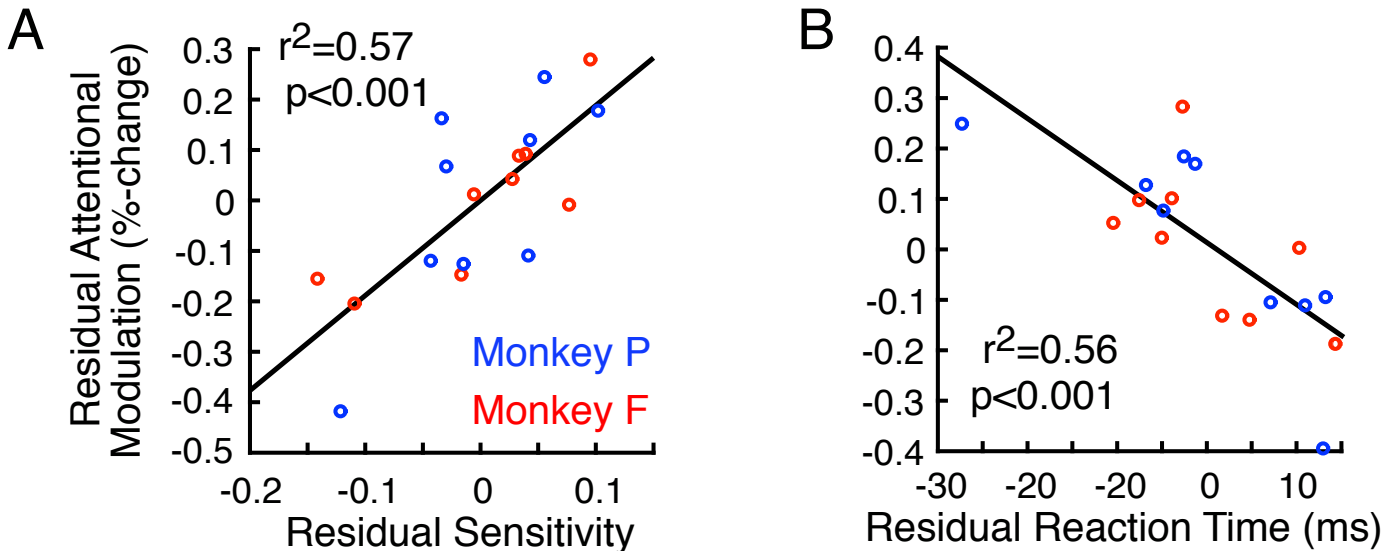


Figure 7

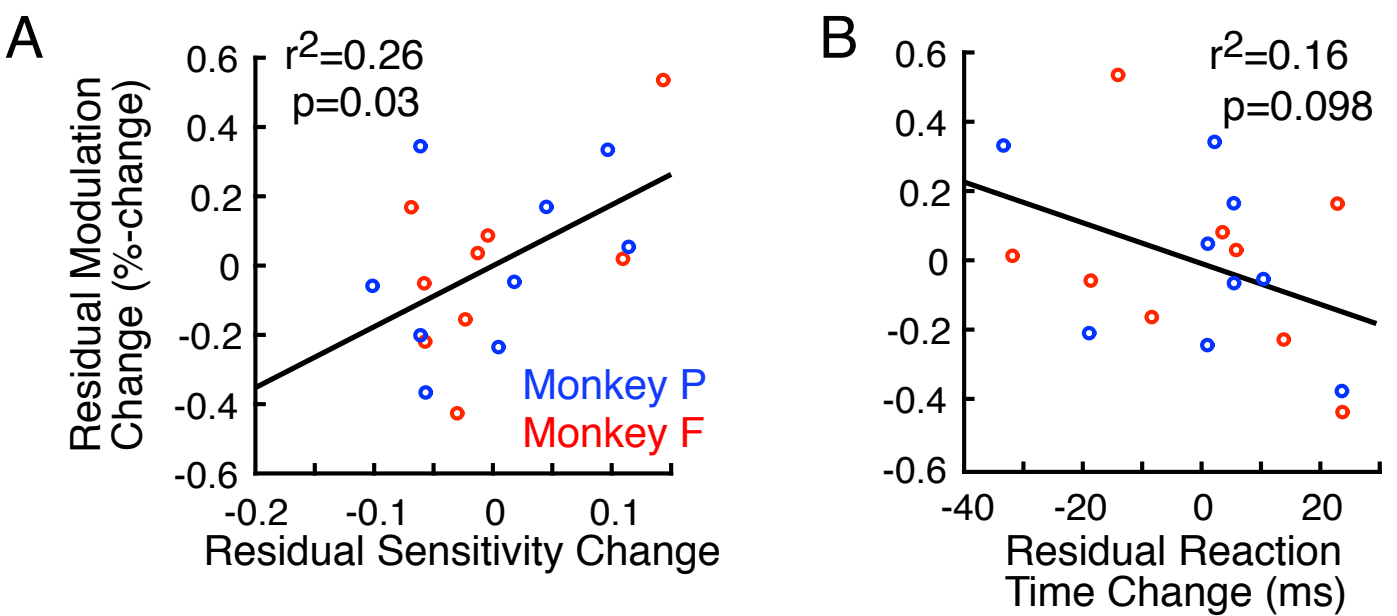


Figure 8